Electronic Supplementary Material (ESI) for CrystEngComm.
This journal is © The Royal Society of Chemistry 2018

Supplementary Information

Expanding Possibilities for Solid-Phase Crystallization by Exsolving Tunable Pd-Ni Core-Shell Nanostructures

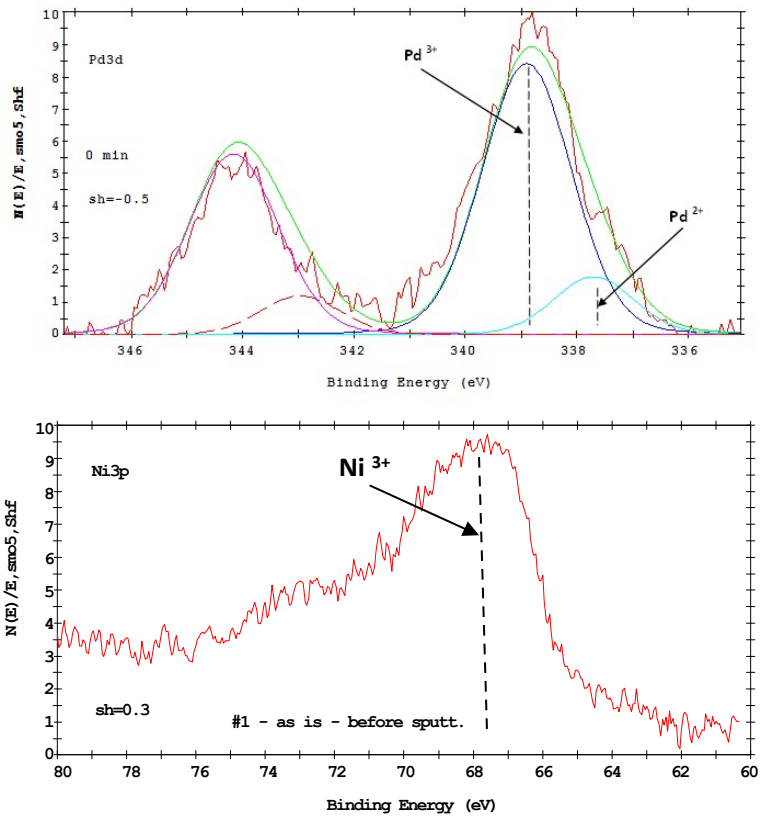

Figure S1. High-resolution (core-level) XPS of the Pd 3d and Ni 3p electron. Deconvolution and integration shows that the 80% of the palladium is in a 3+ valency, while the remainder is in a 2+ valency. XPS of the Ni 3p electron indicates that it is all present in a 3+ state.

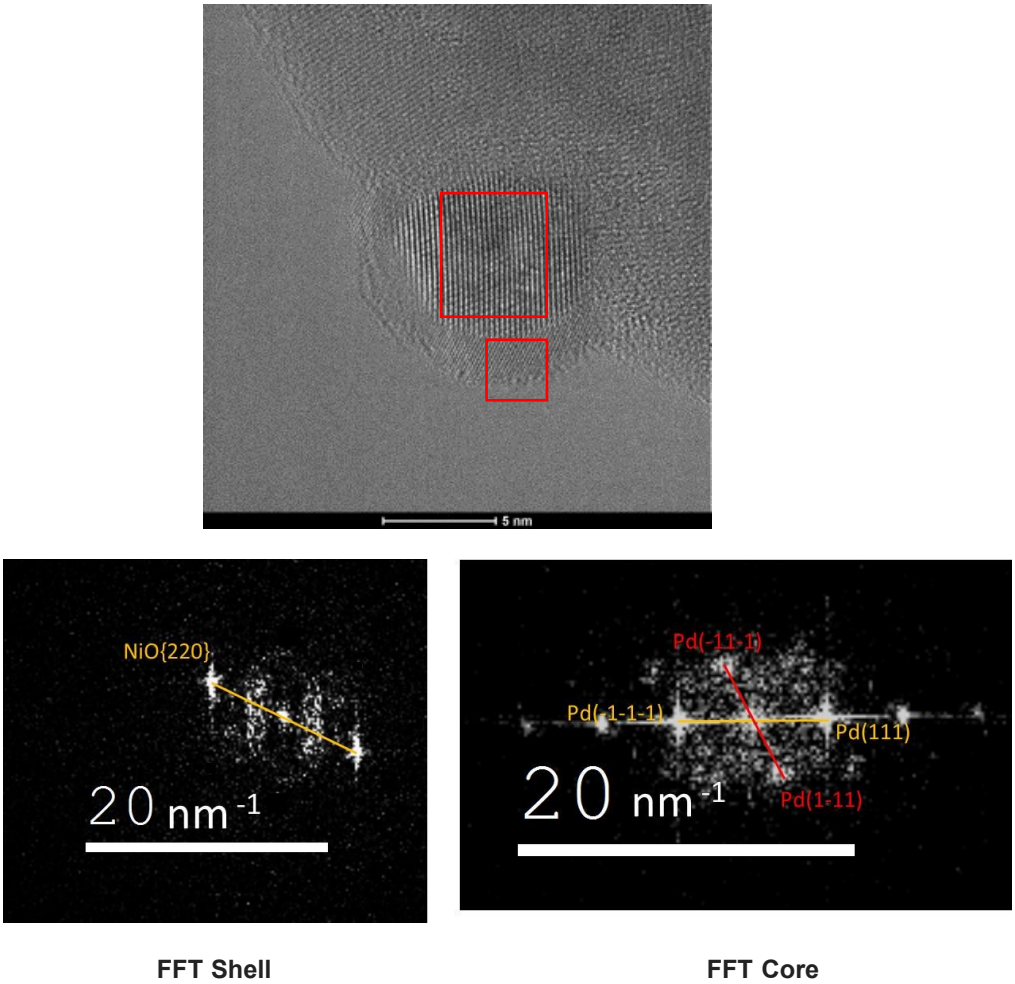

Figure S2. HR-TEM image of core shell from manuscript with lattice fringe measurements using FFT analysis. The fringes in the shell correspond to NiO(220) while the core corresponds to Pd{111}. NiO fringes in the core-FFT are also visible due to the geometry of core-shell particles.

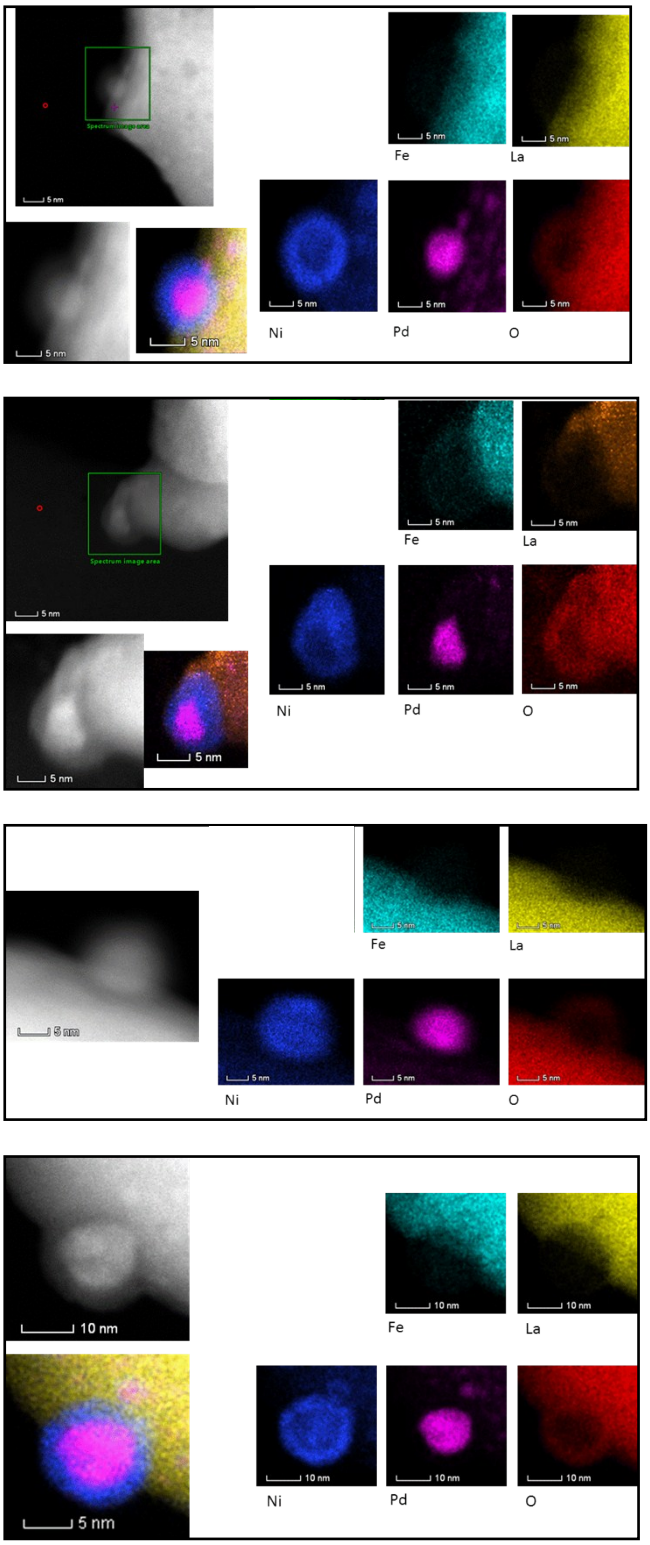

Figure S3. STEM-EDX mapping of Fe, La, Ni, Pd, and O for 4 different particle locations.

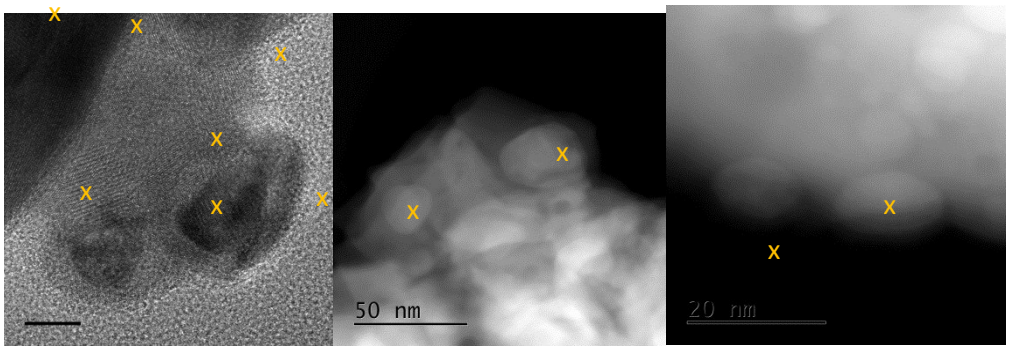

Figure S4: Low-magnification dark/bright field TEM imaging intending to show the relative spacing and population density of core-shell nanoparticles exsolved from the sample. Yellow 'x' indicates Pd-core.

Table S1: Surface (XPS) Ni:Pd as ratio of reduced $LaFe_{0.6}Ni0.3Pd_{0.1}O_{3-\delta}$ as a function of sputter time (~1nm/min)

Sputter time (min)	0	1.5	2.0	2.5	3.0	4.0	8.0
Ni:Pd	13.7	8.0	6.2	5.7	3.9	4.0	3.8

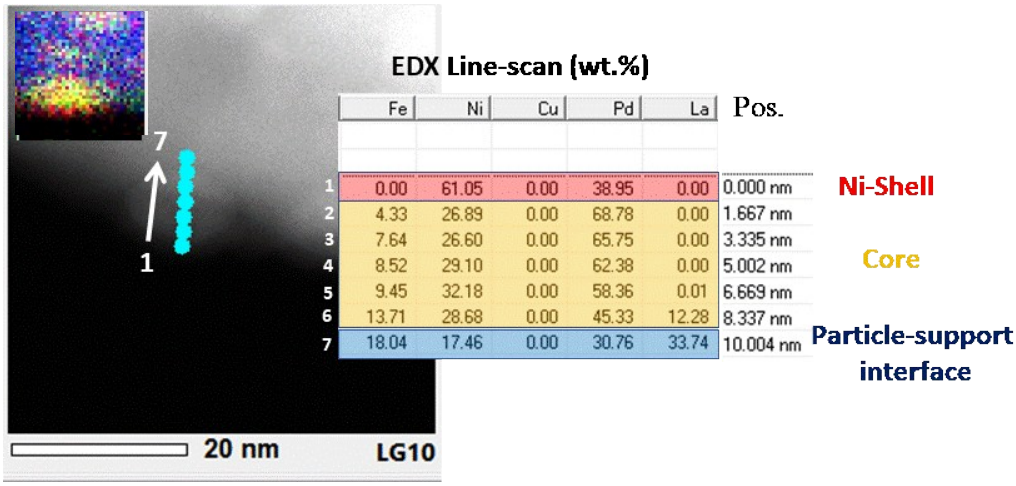

Figure S5. EDX elemental linescan of reduced $LaFe_{0.65}Ni_{0.25}Pd_{0.1}O_{3-\delta}$

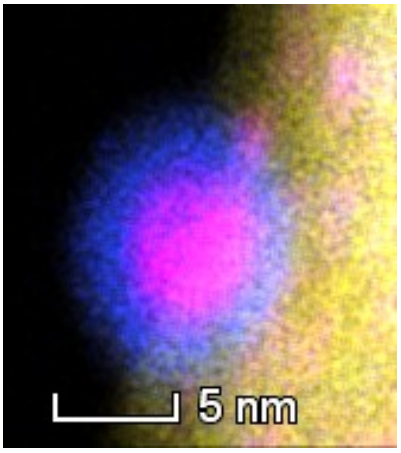

Figure S6: XRD pattern of $LaFe_{0.6}Ni0.3Pd_{0.1}O_{3-\delta}$ reduced at 500 degrees Celsius showing evidence of Pd-only core formation (see mostly-pink structures in the support)

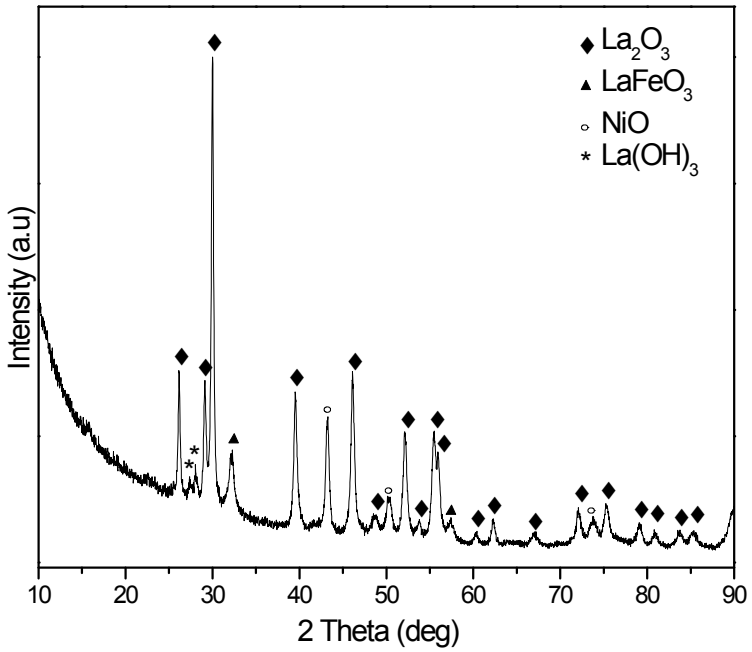

Figure S7: XRD pattern of reduced $LaFe_{0.6}Ni0.3Pd_{0.1}O_{3-\delta}$ giving rise to a support composed of both $LaFeO_3$ and La_2O_3.

Experimental Methods

The catalyst precursors were prepared by sol-gel. Stoichiometric amounts of $La(NO_3)_3 \cdot 6H_2O$, $Ni(NO_3)_2 \cdot 6H_2O$, $Fe(NO_3)_3 \cdot 9H_2O$ and $Pd(NO_3)_2 \cdot H_2O$, respectively for desired composition, were fully dissolved in 5 mL Milli-Q water using sonication bath for 5 min. Afterwards, citric acid and ethylene glycol were added in excess as complexing agents into the solution and sonication repeated for another 5 min. The molar ratio of total cations, citric acid and ethylene glycol was 1:3:3. The obtained solution was heated to 130°C and stirred until gel-like material was formed. Following, the temperature was reduced to 100°C and kept overnight to remove remain solvent and to form foam-gel. Afterwards, the dry foam-gel was grained until a fine powder was formed. Finally, the powder was calcined in air atmosphere at 400°C for 2 h and then at 750°C for 6 h at the rate of 10°C/min to obtain solid-phase-crystallization of perovskite structure precursors. After calcination, the powder was ground again.

Temperature programmed reduction (TPR) was performed on ChemBET-3000 Quantachrome instruments. Prior to TPR measurement, degaussing procedure was submitted on the sample in order to remove any impurities. The degaussing procedure occurred in mixture of 80%He and 20%N_2 (carrier gas) and pure N_2 (calibration/ titration gas) atmosphere for 2h at 200°C and then cooled down to room temperature. For TPR measurement, 70 mg of sample was inserted into cell sample quartz TPR-TPD tube. Each sample was tested as follows: First, fresh sample was reduced at hydrogen atmosphere (mixture of 5%H_2 and 95%N_2) while temperature of furnace was increased at a heating rate of 10°C/min to 800°C. Second, the sample cooled down to room temperature at inert atmosphere in the presence of both mixture of 80%He and 20%N_2 and pure N_2.

The X-ray diffraction (XRD) measurements were taken in Bruker AXSA D8 Advance with CuKα (λ = 1.5406 Å) radiation source and analyzed using Diffrac.EVA software by Bruker. Signals were collected in 2θ range of 10˚ to 100˚ with step-size of 0.005˚, counting times of 0.5 sec and sample rotation rate 15 rpm.

XPS measurements were performed in UHV (2.5×10^{-10} Torr base pressure) using 5600 Multi-Technique System (PHI, USA). The sample was irradiated with an Al K_α monochromated source (1486.6 eV) and the ejected electrons were analyzed by a spherical capacitor analyzer using the slit aperture of 0.8 mm. Sample charging during measurements was compensated with a charge Neutralizer: C1s at 285 eV was taken as an energy reference. Samples were analyzed at the surface and after several steps of sputtering with 4 kV Ar^+ Ion Gun (sputter rate was 11.4 Å/min on SiO_2/Si calibration sample).

Transmission electron microscopy (TEM) images in Figure 2 were taken by Field Emission TEM (Tecnai@ F20, Philips) operated at 200 kV. Analytical TEM images in Figure 3 were taken using a JEOL JEM-2100F microscope operating at accelerating voltage of 200 kV equipped with GATAN 894 US1000 camera. Energy dispersive spectroscopy (EDS) point analysis and mapping were performed using a JEOL JED-2300T energy dispersive X-ray spectrometer. The samples were tilted in 10˚. Probe tracking (drift correction) allowed chemical analysis at the nanometer scale. JEOL Analytical Station software (v. 3.8.0.21) was used for the EDS data analysis. The quantitative analysis was performed by the standard less Cliff−Lorimer method. All scanning TEM (STEM) images were taken in high-angle annular dark-field (HAADF) mode using GATAN 806 HAADF STEM detector. The high-resolution transmission electron microscopy (HRTEM) image and high-angle annular dark-field scanning transmission electron microscopy (HAADF-STEM) image in Figure 1 were acquired using a monochromated and double corrected Titan Themis G2 60-300 (FEI /Thermo Fisher) operated at 200 kV and equipped with a DualX detector (Bruker). The quantitative analysis of the EDS maps was done using the Velox software (FEI / Thermo Fisher).